SPRAY CHARACTERISTICS OF A HYBRID TWIN-FLUID PRESSURE-SWIRL ATOMIZER

M.J. Durham*, P.E. Sojka†, and C.B. Ashmore‡
Purdue University
West Lafayette, IN 47907-2088
Tel: 765-494-1536
Fax: 765-494-0530
Email: mjdurham@purdue.edu; sojka@ecn.purdue.edu

ABSTRACT

The spray performance of a fuel injection system applicable for use in main combustion chamber of an oxidizer-rich staged combustion (ORSC) cycles is presented. The experimental data reported here include mean drop size and drop size distribution, spray cone half-angle, and momentum rate (directly related to spray penetration). The maximum entropy formalism, MEF, method to predict drop size distribution is applied and compared to the experimental data. Geometric variables considered include the radius of the injector inlet orifice plate through which oxidizer flows (R_0) and the exposed length from the fuel inlet to the injector exit plane (L_2). Operating conditions that were varied include the liquid mass flow rate and air mass flow rate. For orifices B and C there is a significant dependence of D_{32} on both the air and liquid mass flow rates, as well as on L_2. For the A orifice, the momentum rate of the air flow appears to exceed a threshold value above which a constant D_{32} is obtained. Using the MEF method, a semi-analytical process was developed to model the spray distribution using two input parameters ($q = 0.4$ and D_{q0}). The momentum rate of the spray is directly related to the air and liquid mass flow rates. The cone half angle of the spray ranges from 25 to 17 degrees. The data resulting from this project will eventually be used to develop advanced rocket systems.

INTRODUCTION

The goal of this study was to further our understanding of a candidate fuel injection system in the main combustion chamber of oxidizer rich staged combustion (ORSC) cycles. To that end, a hybrid twin-fluid pressure-swirl atomizer with axial gas flow and swirling liquid flow was fabricated and tested. This design is believed to approximate that of existing injector designs[1], for which little is known outside the fact that gaseous oxidizer flows down the center of the atomizer and that the fuel is injected tangentially forming a swirling film.

An understanding of this injector's performance was developed by measuring the effects of varying atomizer geometry and mixture ratio (air to liquid mass flow rate ratio, or ALR) on spray formation (reported here as mean drop size, drop size distribution, and spray cone half-angle). This information will be used to design hybrid twin-fluid pressure-swirl injectors that have a maximized efficiency and longevity.

LITERATURE REVIEW

The fuel injector investigated during this study was designed to functionally match that of Cohn *et al.*[1] and a design from the patent literature[2]. Though successfully used by other nations, this injector type is fairly new to the United States so little existing literature is available.

At first glance, this injector seems to share characteristics of both pressure-swirl and twin-fluid atomizers. However, upon closer inspection one can see that it is different from both generic designs in several important ways:

- It will not behave as a pressure-swirl atomizer because (i) there is a considerable mass flow of gas down the centerline, and (ii) there is no contraction at the exit orifice;
- The design differs from a twin-fluid atomizer in that (i) there is a shroud to shield the liquid film from the atomizing air for a portion of the flow path, and (ii) the liquid film has a swirling component.

While there is little data describing the quantitative performance of this injector type, a basic understanding of twin-fluid swirling atomizers suggests the following quantities will play a role in determining their performance: ALR, geometrical design parameters R_2, R_1, R_0, δ, L_1, and L_2, and either liquid or air mass flow rate. In this

* Graduate Research Assistant, School of Mechanical Engineering
† Profesor, School of Mechanical Engineering
‡ Undergraduate Research Assistant, School of Mechanical Engineering

paper we present only the influence of geometric parameters R_0 and L_2, along with the air and liquid mass flow rates.

EXPERIMENTAL APPARATUS

The geometry tested is shown in Figure 1. Two geometric values were varied during these tests. R_0 was chosen in an attempt to decouple combustion instabilities from the upstream oxidizer flow. Since it is theorized that wave instabilities cause drop formation directly from the swirling film then varying the length of the two-phase interaction length L_2 should help us understand what role these instabilities play in injector performance.

A shorthand notation was developed for recording the atomizer geometric setup. The letters A, B, and C are used to differentiate between various values of R_0. The letters X, Y, and Z are used to track the length of the two-phase flow, L_2. See Table 1.

The baseline injector was designed for an ALR of λ and a gas velocity of v m/s to match previous units of similar design. Water was used in place of fuel and air in place of oxygen for all tests.

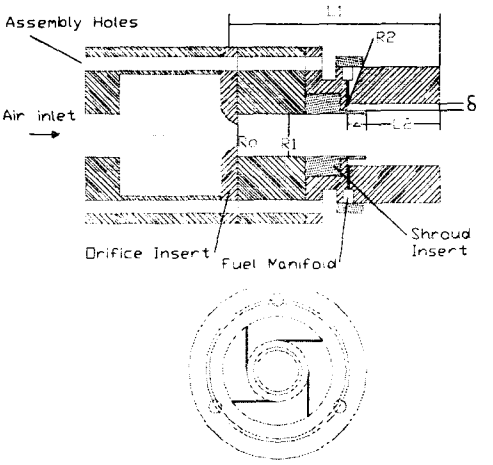

Figure 1: Atomizer Schematic

Table 1: Orifice and Shroud Dimensions

Orifice Insert	Radius R_0 (mm)	Shroud Insert	Two-phase flow length L_2 (mm)
A	R_0	X	$4L_2$
B	$1.5R_0$	Y	$2L_2$
C	$2.5R_0$	Z	L_2

Three types of measurements were made: drop size distribution, cone angle, and momentum rate. Testing was performed for a range of air-to-liquid ratios by mass ($0.375\lambda < ALR < 1.15\lambda$) and nine geometric configurations (AX, AY, AZ, BX, BY, BZ, CX, CY, and CZ). ALR was varied by adjusting the mass flow rates of the air (0.86α, α, and 1.14α) and water (0.6ω, ω, and 1.4ω).

Drop size data were obtained using a Malvern 2600 spray analyzer. This instrument measures the diffraction of light by drops in the spray as they pass through the instrument laser beam. The collecting lens focal length was 300 mm, which gives a drop size sampling range between 5.6 and 564 μm. The model-independent mode of data reduction was employed, with data acquired perpendicular to the centerline of the injector at an axial distance of 15 cm downstream of the exit orifice.

Spray cone angles were calculated from digital pictures (Sony MVC FD95) using simple geometry. They are reported as half-angles, with an experimental uncertainty of ±4 degrees. Figure 2 shows a typical spray pattern.

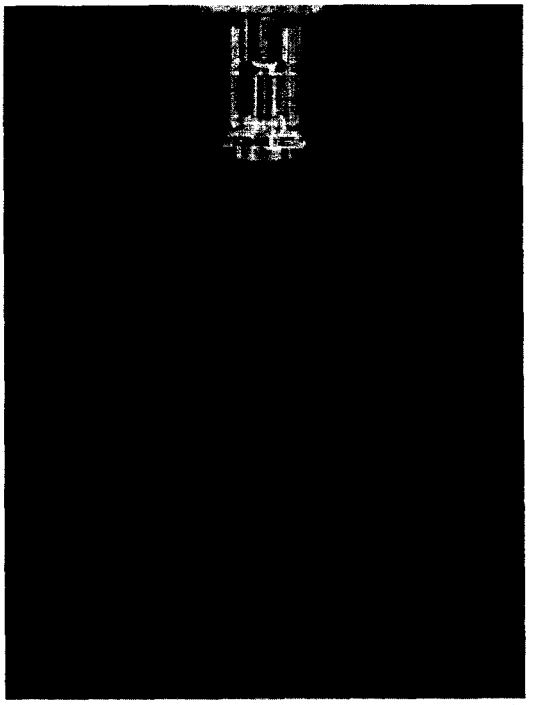

Figure 2: Representative spray formation image.

A limited amount of momentum rate data was obtained using the momentum rate probe developed by Bush *et al.*[3]. The probe was placed 6 mm from

the exit orifice of the injector. Experimental uncertainty is estimated to be ±50 mN.

RESULTS AND DISCUSSION

It is theorized that the atomization process starts with wave instabilities, which depend on the relative velocity between the air and water. With increasing relative velocity the wavelength of the instability will decrease, which would lead to finer drops. Drop size is also expected to depend on the thickness of the liquid film near the atomizer exit plane; a smaller liquid film thickness should result in a smaller D_{32} value. Since an increase in ALR should result in a reduction in film thickness, an increase in ALR is expected to decrease D_{32}.

Figures 3 through 8 show D_{32} as a function of water mass flow rate for three air mass flow rates. Each figure contains two atomizer geometric configurations for comparison. In all cases uncertainty bars represent one standard deviation of statistical variation in the data. Figures 3 through 5 illustrate the two extremes of two-phase region length, the longest shroud insert, Z, and the shortest insert, X. This corresponds to the shortest two-phase flow interaction length L_2 and the longest two-phase flow interaction length, respectively. Figures 6 through 8 illustrate the effect of orifice diameter (R_0) on drop formation.

Figure 3 shows mean drop size to be fairly independent of ALR for this geometry, with the only noticeable change for both geometries occurring at the lowest air flow rate. The significant change in D_{32} comes when the length of the two phase flow region, L_2, is varied; as might be expected increasing the two-phase flow length decreases D_{32} because the liquid is exposed to aerodynamic shear for a greater distance.

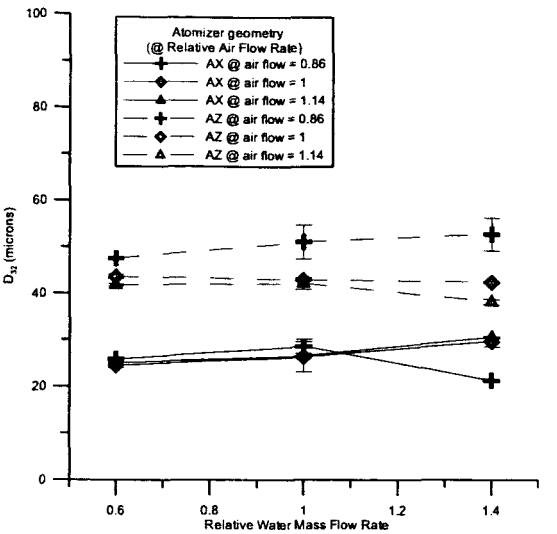

Figure 3: The influence of two-phase flow interaction length on D_{32} versus water mass flow rate behavior for three air mass flow rates.

In Figure 4, we see that at lower water mass flow rates the longer two-phase flow interaction length leads to smaller drops, as anticipated. However, as the liquid mass flow rate increases the D_{32} values for the two L_2 cases converge toward a common value. Surprisingly, at the maximum liquid mass flow rate the shorter L_2 case yields a smaller D_{32} value than the longer L_2 case. Observe, however, that the ALR for this behavior (0.52 λ) is well outside the ALR value for which the atomizer was designed (λ). Even with that said, this behavior was not predicted. Further experiments are required to understand this behavior since no consistent explanation is available at this time.

The qualitative D_{32} versus liquid mass flow rate behavior in Figure 5 is the same as that in Figure 4 for both two-phase interaction lengths. However, in contrast to Figure 4 only the longer two-phase interaction length data exhibits the substantial increase in D_{32} with an increase in liquid mass flow rate which causes the X case D_{32} value to exceed its Z counterpart at the highest liquid mass flow rate considered (1.4ω). One explanation for this observation is that the longer two-phase flow region provides more time for droplet coalescence so this phenomenon becomes significant. With the shorter mixing region, coalescence wouldn't have time to develop before the drops exit the atomizer.

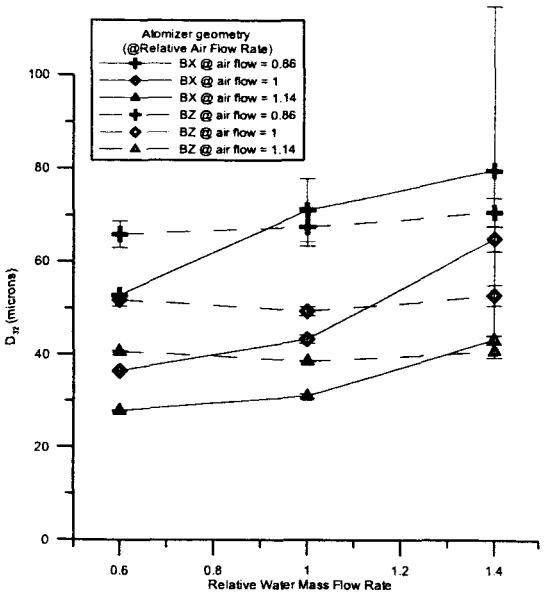

Figure 4: The influence of two-phase flow interaction length on D_{32} versus water mass flow rate behavior for three air mass flow rates.

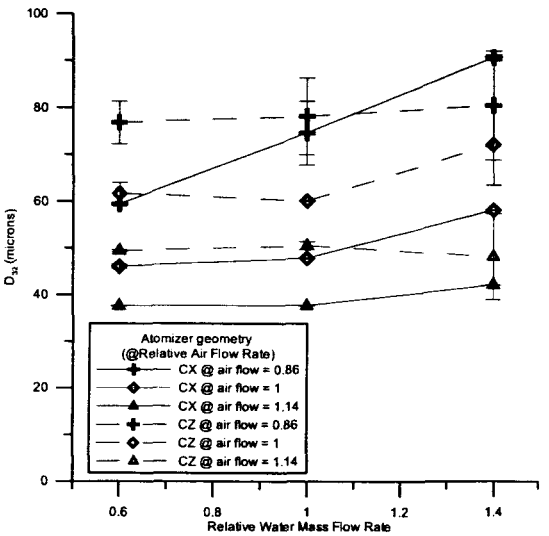

Figure 5: The influence of two-phase flow interaction length on D_{32} versus water mass flow rate behavior for three air mass flow rates.

Figures 6 through 8 illustrate the influence of orifice diameter on mean drop size versus water mass flow rate behavior. Here, we see that increasing the orifice diameter changes both the quantitative and qualitative results. First, increasing the orifice diameter from A to C always leads to an increase in D_{32}, regardless of liquid and air mass flow rates or two-phase flow interaction length. Second, when the orifice diameter is A there is little effect of either liquid mass flow rate or air mass flow rate on D_{32}, again regardless of the two-phase flow interaction length (the most noticeable variation occurs for a two-phase flow interaction length of Z and there the data lie within the sum of their experimental uncertainties). However, when the orifice diameter is increased to C, increasing the air mass flow rate leads to a significant decrease in D_{32}, regardless of liquid mass flow rate or two-phase interaction length.

Our hypothesis is that there is a threshold momentum rate for air inside the atomizer that, once exceeded, controls spray formation. In effect, there is an "excess" air momentum rate in these cases. In contrast, when the air momentum rate falls below this threshold value spray formation is controlled by both air and liquid momentum rates with an increase in air momentum rate causing a decrease in D_{32}. We do note, however, that for the X two-phase flow interaction length there is also an effect of liquid momentum rate. We have no explanation for that behavior at this time.

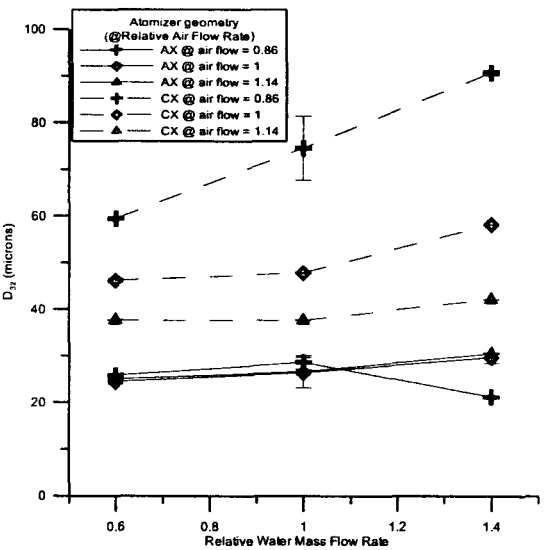

Figure 6: The influence of exit orifice diameter on D_{32} versus water mass flow rate behavior for three air mass flow rates.

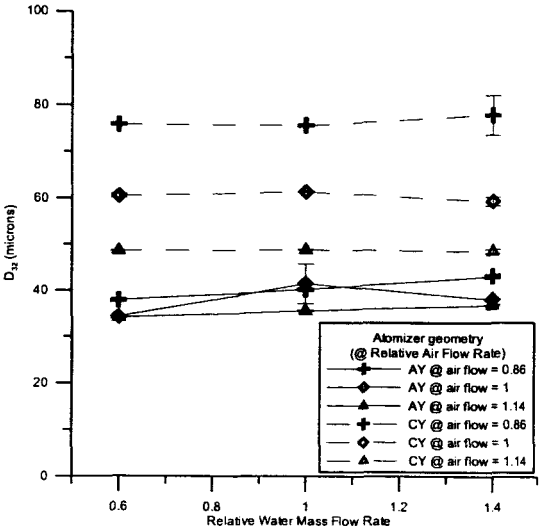

Figure 7: The influence of exit orifice diameter on D_{32} versus water mass flow rate behavior for three air mass flow rates.

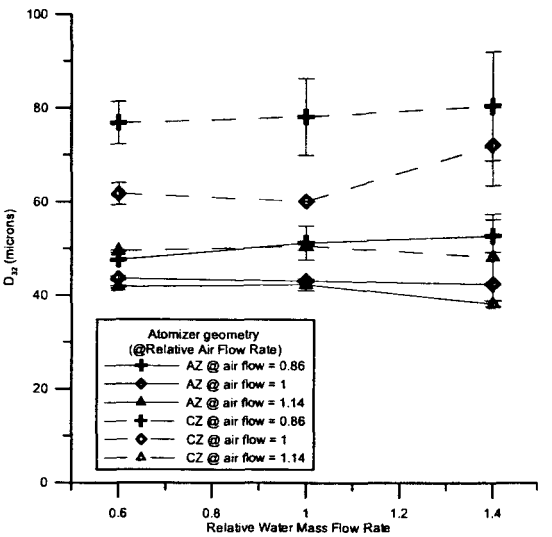

Figure 8: The influence of exit orifice diameter on D_{32} versus water mass flow rate behavior for three air mass flow rates.

A drop size distribution can not be totally described by just one parameter. Some measure of both the width and the peak of the distribution must be provided to get a complete description. Therefore, two parameters are needed to completely describe the distribution. Two approaches to model distributions have been described by Babinsky and Sojka[4], discrete probability function(DPF) and maximum entropy formalism[5](MEF). DPF is applicable only to primary atomization dominated spray formation processes. Since the Weber number for this atomizer has a minimum value of 40, secondary atomization is present making the DPF method non-applicable.

Using the MEF method, a program was written to determine the drop size distribution using two input parameters. The program uses the peak of the drop size distribution as an input and then solves equation (1) for incremented values of q.

$$f_3 = \frac{q^{q-4}/q \cdot e^{-\frac{\left(\frac{D}{D_{qo}}\right)^q}{q}}}{\Gamma\left(\frac{4}{q}\right) \cdot D_{qo}^4} \cdot D^3 \qquad (1)$$

The peak of the distribution, D_{qo}, was chosen as an input because it is easily attained from experimental data. The test matrix incremented q by 0.1 from 0.1 to 1.0 and by 1 from 1 to 10. A value of q was then chosen which results in a curve that most closely matched the experimental data. The degree of matching is evaluated using the parameter R^2. For most of the sixteen different cases tested, the best value of q was 0.4 or 0.5 with an R^2 value of 0.9 or greater, see Table 2.

Table 2: Results from MEF analysis

m_{liq}	m_{air}	R_0	L_2	q (D_{max})	R^2 (D_{max})
0.6	0.86	A	X	0.40	0.93
0.6	1.14	A	X	0.50	0.93
1.4	1.14	A	X	0.40	0.93
0.6	0.86	A	Z	0.40	0.95
0.6	1.14	A	Z	0.30	0.94
1.4	0.86	A	Z	0.40	0.89
1.4	1.14	A	Z	0.40	0.88
0.6	0.86	C	X	0.40	0.96
0.6	1.14	C	X	0.70	0.82
1.4	0.86	C	X	0.20	0.77
1.4	1.14	C	X	0.40	0.94
0.6	0.86	C	Z	0.60	0.73
0.6	1.14	C	Z	0.40	0.93
1.4	0.86	C	Z	0.50	0.31
1.4	1.14	C	Z	0.20	0.39

Using a value of q equals 0.4 and the peak of the distribution as the two inputs, we have a semi-analytical method to model the spray distribution. Figures 9 and 10 display the results for the A and C orifices, respectively. Each graph shows two curves, one for X and one for Z. The experimental distributions are also plotted in the figures for direct comparison with the uncertainty bars representing one standard deviation.

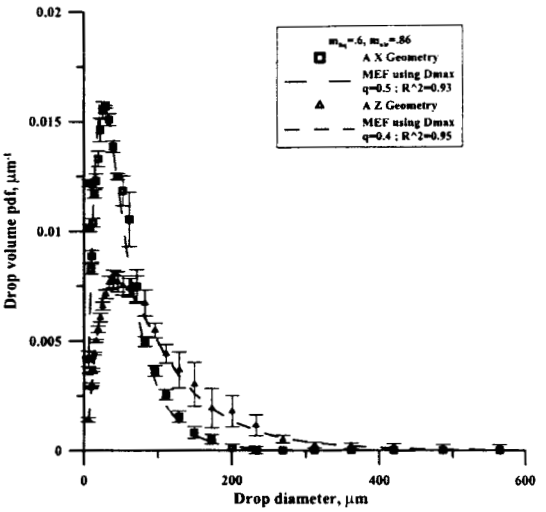

Figure 9: Representative result of MEF method

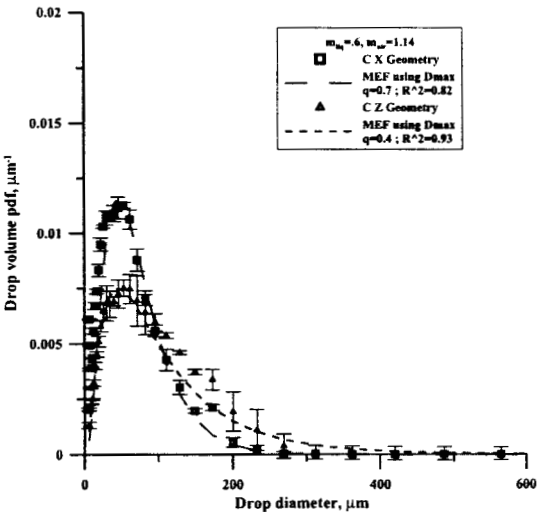

Figure 10: Representative result of MEF method

Figure 11 presents representative spray momentum rate data for geometry BY. All liquid and air mass flow rates were considered. As expected, increases in either air or water mass flow rate lead to an increase in momentum rate. Consequently, spray penetration (and perhaps mixing at the local level) is enhanced as either liquid or air mass flow rate rises.

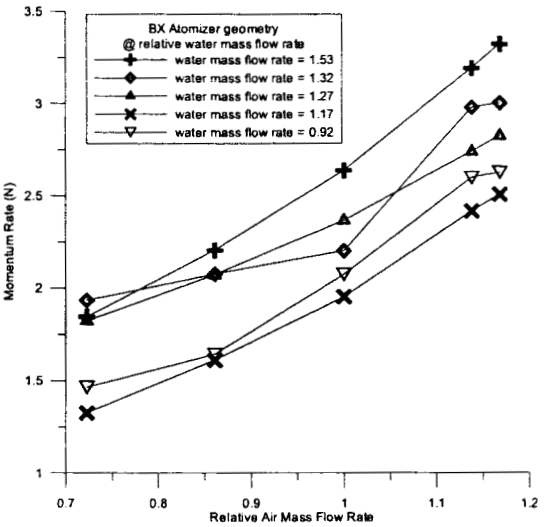

Figure 11: Momentum rate versus air mass flow rate for five liquid flow rates and one atomizer geometry (BX).

Selected cone angle data are shown in Table 3. Results are presented as cone half-angle versus air mass flow rate for a single liquid mass flow rate (nominally 0.88ω) when using the BY geometry. As expected, increasing the air mass flow rate decreases the spray cone half-angle. This finding indicates that spray dispersion will most likely diminish as air mass flow rate increases.

Table 3: Cone Angle Data

Air mass flow rate	Liquid mass flow rate	Spray cone half-angle, degrees
0.72α	0.88ω	25±4
0.86α	0.88ω	21±3
1.00α	0.88ω	21±3
1.07α	0.88ω	17±3
1.14α	0.96ω	17±3

SUMMARY AND CONCLUSIONS

In summary, for orifices B and C there is a significant dependence of D_{32} on both the air and liquid mass flow rates, as well as on L_2. As expected, an increase in air mass flow rate decreases D_{32} while increasing the liquid mass flow rate increases D_{32}. Increasing L_2 also decreases D_{32}, as long as the liquid mass flow rate is low. However, the injector exhibits peculiar behavior at higher mass flow rates when comparing the affect of L_2 on D_{32}. The longer two-phase interaction length gives larger mean drop sizes. The reason for this behavior is currently unknown, although droplet coalescence may play a role.

For the A orifice the momentum rate of the air flow appears to exceed a threshold value above which a constant D_{32} is obtained. However, an increase in L_2 leads to the expected decrease in mean drop size, though on a much smaller scale than with the other geometries. Using the A orifice creates a small (30- 50 μm) and consistent (std dev) spray pattern, regardless of mass flow rates. It's hypothesized that the small orifice creates a highly turbulent air flow. This higher degree of turbulence dominates the atomization process much more than with larger R_0 diameters.

Using the MEF method, a semi-analytical process was developed to model the spray distribution. Two parameters are needed for this method. First, q ,which was shown to be 0.4 in most cases. Second, the peak of the distribution, chosen because it is easily attainable through experiments. With these two inputs, a drop size distribution can be modeled completely.

The momentum rate of the spray is directly related to the air and liquid mass flow rates. An increase in either results in an increase in spray momentum. Consequently, spray penetration (and perhaps mixing at the local level) is enhanced as either liquid or air mass flow rate rises.

The cone half angle of the spray ranges from 25 degrees for an air mass flow rate of 0.72α and decreases to 17 degrees for an air mass flow rate of 1.14α. This finding indicates that spray dispersion will most likely diminish as air mass flow rate increases.

REFERENCES

[1] Cohn, R.K., Strakey, P.A., Muss, J.A., Johnson, C.W., Bates, R.W., and Talley, D.G., "Swirl Coaxial Injector Development", AIAA Paper 2003-0124, 41st AIAA Aerospace Sciences Meeting and Exhibit, Reno, NV, Jan. 6-9, 2003.

[2] Vasin, A.A., Kamensky, S.D., Katorgin, B.I., Kolesnikov, A.I., Nosov, V.P., Stavrulov, A.I., Fedorov, V.V., and Chvanov, V.K., United States Patent, US 6,244,041, B1 Jun. 12, 2001.

[3] Bush, S.G., Bennett, J.B., Sojka, P.E., Panchagnula, M.V., and Plesniak, M.W., "A Momentum Rate Probe For Use With Effervescent Sprays," Review of Scientific Instruments, **65(5)**, 1878-1885 (1996).

[4] Babinsky, E., Sojka, P.E., Modeling drop size distributions, Progress in Energy and Combustion Science 28 (2002) 303-329.

[5] Cousin, J., Yoon, S.J., Dumouchel, C., Coupling of Classical Linear Theory and Maximum Entropy Formalism for Prediction of Drop Size Distribution in Sprays: Application to Pressure-Swirl Atomizers. Atom Sprays 1996;6:601-22